


Cite this: *RSC Pharm.*, 2025, **2**, 1175

# Clobetasol propionate and pramoxine hydrochloride loaded nanolipid carrier gel for the treatment of atopic dermatitis†

Akhil Suresh,<sup>a</sup> K. V. Navyasree,<sup>b</sup> M. S. Sreelakshmi<sup>a</sup> and Vidya Viswanad \*<sup>a</sup>

**Aim.** To prepare and evaluate clobetasol propionate (CP) and pramoxine hydrochloride (PH) loaded nanolipid carrier (NLC)-based gel for improved skin permeation in the treatment of atopic dermatitis. **Methodology.** CP and PH-loaded NLCs were prepared by the melt emulsification ultrasonication technique. *In vitro*, *ex vivo*, and *in vivo* studies in the atopic dermatitis animal model of formulated drug-loaded NLC (DNLC) gel were evaluated. Dermal pharmacokinetic parameters were evaluated by Phoenix WinNonlin software. **Results and discussions.** DNLC gel was prepared successfully. Skin permeation and retentive property of the DNLC gel showed that CP from the DNLC had a permeability flux of  $5.88 \mu\text{g cm}^{-2} \text{h}^{-1}$  and an enhancement ratio of 1.92 compared to a CP drug solution, while PH from the DNLC gel had a permeability flux of  $9.52 \mu\text{g cm}^{-2} \text{h}^{-1}$  and an enhancement ratio of 1.62 compared to a PH drug solution. Dermal pharmacokinetic parameters were determined using WinNonlin software. CP retention at 24 h in stratum corneum, epidermis, and dermis was  $4.25 \pm 0.02 \mu\text{g}$ ,  $75.77 \pm 0.01 \mu\text{g}$ , and  $32.04 \pm 0.012 \mu\text{g}$ , respectively, while PH retention at 24 h was  $11.82 \pm 0.003 \mu\text{g}$ ,  $344.0 \pm 0.05 \mu\text{g}$ , and  $172.85 \pm 0.040 \mu\text{g}$ , respectively. More CP was retained from the DNLC gel than that from marketed CP cream. *In vivo* animal studies confirmed the effectiveness of DNLC gel in treating atopic dermatitis compared to commercial cream and individual drug-loaded DNLC gel, decreasing induced disease on a par with marketed CP cream. Epidermal thickness, immunoglobulin E (IgE), and absolute eosinophil count (AEC) showed the greatest reduction in the DNLC gel treatment group.

Received 18th February 2025,  
Accepted 19th July 2025

DOI: 10.1039/d5pm00048c

rsc.li/RSCPharma

## 1. Introduction

Atopic dermatitis (AD) is a chronic relapsing skin disease characterized by severe itching, dry skin, and local skin inflammation affecting 15–20% of children and 1–3% of adults worldwide. The disease has a distinct acute and chronic phase that differs in histological and immunological profile.<sup>1</sup> The prevalence of eczema and other allergic symptoms is increasing globally, especially among children, making AD a significant global concern.<sup>2</sup> The condition often relapses and requires long-term management, significantly impacting the

quality of life of individuals.<sup>3</sup> Notably, AD frequently marks the beginning of the atopic march, causing patients to be more susceptible to developing allergic rhinitis and asthma due to immune sensitization and impaired skin barrier.<sup>4</sup> AD is influenced by genetic, immunologic, and environmental factors, making it a complex pathological condition that requires timely intervention to prevent further progression. Understanding its complex pathophysiology opens new avenues for treatment and management of the condition.<sup>5</sup> Innovative topical treatments, such as silver-nanolipid complexes, have shown promise by combining antimicrobial action with barrier-restoring properties.<sup>6</sup> Microemulsion-based gels and nanoparticles have demonstrated improved delivery and efficacy of corticosteroids like clobetasol propionate, offering potential for enhanced treatment outcomes.<sup>7–9</sup> The heterogeneous signs and triggers of AD underscore the need for personalized management strategies and proactive treatment approaches.<sup>10,11</sup>

Topical calcineurin inhibitors and corticosteroids are part of current therapeutic options; however, their use has been limited due to various drawbacks, such as burning sensation,

<sup>a</sup>Department of Pharmaceutics, Amrita School of Pharmacy, Amrita Vishwa Vidyapeetham, Amrita Institute of Medical Sciences Health Science Campus, AIMS Ponekkara P.O., Kochi, Kerala-682041, India.

E-mail: vidyaviswanad@aims.amrita.edu; Tel: +919495934892

<sup>b</sup>Department of Pharmacology, Amrita School of Pharmacy, Amrita Vishwa Vidyapeetham, Amrita Institute of Medical Sciences Health Science Campus, AIMS Ponekkara P.O., Kochi, Kerala-682041, India

† Electronic supplementary information (ESI) available. See DOI: <https://doi.org/10.1039/d5pm00048c>



redness, and allergic responses. Additionally, the main concern has been systemic absorption, which can lead to breathing difficulties, facial swelling, and a systemic immune-suppressive impact, all of which increase the risk of malignancies.<sup>12,13</sup> Menthol, pramoxine, and capsaicin are compounds that function as local numbing medications to temporarily block the transmission of itch signals from the skin to the central nervous system.<sup>14</sup> Pramoxine belongs to the class of drugs known as local anesthetics and works by numbing the skin to block pain and itch sensations.<sup>15</sup>

The use of permeation enhancers in topical vehicle systems improves medication penetration over the skin; however, the use of such chemical enhancers may be detrimental, as many are irritants.<sup>16</sup> As a result, a topical carrier free of chemical enhancers to aid medication absorption through the skin is preferred. Colloidal medication delivery techniques are projected to outperform traditional topical administration systems for clobetasol propionate (CP). Solid lipid nanoparticles (SLNs), microspheres, lipid nanocarriers, lecithin/chitosan nanoparticles, and microparticulate drug delivery systems have all been designed and tested for the topical administration of CP.<sup>16–18</sup> The use of permeation enhancers in topical vehicle systems enhances drug permeation across the skin, but the employment of such chemical enhancers could be harmful, as many of them are irritants.<sup>16</sup> Therefore, a topical vehicle without chemical enhancers to facilitate drug permeation through the skin is desirable. They offer many advantages, such as not requiring organic solvents during preparation, stability against drug hydrolysis, and relative stability during storage. However, due to their rigid structure, erratic gelation propensity, particle development, and unexpected polymeric transitions, the potential of solid-lipid nanocarriers as drug carriers was restricted by drug expulsion during storage. Nanostructured lipid carriers were developed to address the challenges with solid-lipid nanoparticles. At normal temperatures, the NLCs remain solid, even when a significant amount of liquid lipids is present. Compared to SLNs, the combination of solid and liquid lipids creates a less structured matrix with greater imperfections that can accommodate more drug molecules and achieve higher entrapment efficiency. Additional advantages over SLNs include reduced toxicity, medication protection, and a higher level of stability during storage. NLCs are less prone to have unexpected gelation due to their reduced water content, which is a key concern with SLNs.<sup>19</sup> The ability of nanolipid carriers to exchange lipids with the outermost layer of the stratum corneum after adhering to the skin makes them an attractive choice for topical drug delivery. NLCs are composed of both solid and liquid lipids, resulting in structures with enhanced drug loading, altered drug release patterns, and improved stability features.<sup>20,21</sup> NLCs also significantly improve skin hydration and exhibit occlusive properties due to the reduction in transepidermal water loss; this occlusive trait can aid in skin hydration and medication penetration.<sup>22,23</sup>

CP is a potent corticosteroid that reduces inflammation and redness in inflammatory conditions like eczema and dermatitis.

Pramoxine hydrochloride blocks the voltage-gated sodium channel, thereby reversibly numbing the sensation of itch. The combination of both drugs can provide substantial symptomatic relief by addressing both inflammation and pruritus. Currently, no marketed formulations exist for the combined dosage form of CP and PH. This study aimed to prepare a topical NLC-based gel formulation of CP and PH that can enhance skin retention and permeation and to evaluate its potential in managing AD through an *in vivo* animal study in comparison with a marketed CP cream. The NLCs developed in our previous work were incorporated into Carbopol 934 gel to achieve increased contact time and a consistency suitable for topical application. The prepared DNLC gel was evaluated for physicochemical properties, rheological studies, *in vitro* drug release, *ex vivo* porcine skin permeation, *ex vivo* porcine skin retention, rhodamine-tagged DNLC gel skin permeation studies, and *in vivo* studies on Wistar rats, followed by histopathological investigations and serum IgE and AEC level measurements to assess the disease-mitigating properties of the DNLC gel compared to the marketed formulation of CP, CP-loaded NLC gel, PH-loaded NLC gel, and NLC gel without drug.

## 2. Materials and methods

### 2.1 Materials

Clobetasol propionate was supplied by Mahima Life Sciences, Haryana, India. Pramoxine hydrochloride, triethanolamine, and 2,4-dinitrochlorobenzene were purchased from Sigma-Aldrich Co. LLC. Stearic acid, Tween 80, propylparaben, and propylene glycol were obtained from Nice Chemicals, Kochi. Oleic acid and Carbopol 934 were procured from Loba Chem. Pvt. Ltd, Mumbai. Poloxamer F68 was shipped from Research-Lab Fine Chem Industries, Mumbai. Soya lecithin was obtained from Hi Media Laboratories Pvt. Ltd, Mumbai. Millipore water was used during this study.

### 2.2 Animals

Wistar rats weighing 250 g–300 g were obtained from the central animal house facilities at the Amrita Institute of Medical Sciences and Research Centre (AIMS), Kochi, India. The animals were housed in the central laboratory animal facility, AIMS, under standard laboratory conditions with a 12 hour light/dark cycle at  $25 \pm 2$  °C, provided with standard animal feed and water *ad libitum*. All experimental procedures were approved by the Institutional Animal Ethical Committee (IAEC), AIMS, with ref. no. IAEC/2017/3/18.

### 2.3 Preparation of an optimized drug-loaded nanostructured lipid carrier (DNLC)

Drug-loaded NLCs were prepared and optimized using the melt emulsification ultrasonication technique based on our previous work (Dixit C. Mohan *et al.*, 2018).<sup>24</sup> In brief, oleic acid was used as the liquid lipid and stearic acid as the solid lipid. The required quantities of medicines, liquid lipids, and



solid lipids—constituting the lipid phase—were weighed. The aqueous phase contained surfactants, co-surfactants, stabilizers, and distilled water. After heating both phases in a water bath at 80 °C for 20 minutes, the aqueous phase was added dropwise to the lipid phase on a magnetic stirrer at 750 rpm while maintaining the temperature at 80 °C. The resulting primary emulsion was then subjected to probe sonication at 70% amplitude with 6–2 pulses for 15 minutes, followed by cooling in an ice bath to produce an NLC dispersion.

## 2.4 Characterization of the DNLC

**2.4.1 Particle size and zeta potential.** The particle size, polydispersity index (PDI), and zeta potential of the nanoparticles were measured by dynamic light scattering (Zetasizer Nano ZS, Malvern Instruments Ltd, Malvern, UK). Before measurements, the samples were first diluted with Milli-Q water to measure the particle size and then with conductivity-adjusted Milli-Q water to measure the zeta potential.<sup>24</sup>

**2.4.2 Scanning electron microscopy (SEM).** The surface morphology of the DNLC was examined by SEM (VEGA3 TESCAN) by placing the sample on metal studs with double-sided conductive tape and observed at an accelerated voltage of 20 kV.<sup>23</sup> The DNLC dispersion was diluted with distilled water, after which a drop of this sample was placed on the slide and allowed to dry.

**2.4.3 Transmission electron microscopy (TEM).** To further confirm the morphology of the DNLC, TEM studies were carried out by following a negative staining method using HR-TEM (Tecnai G2F20, Germany) equipped with a CCD camera having 4k × 4k image resolution operating at an accelerated voltage of 200 kV. 5 µL of diluted DNLCs was placed on a carbon-coated copper grid and allowed to dry for 12 h at room temperature.<sup>24</sup>

**2.4.4 Entrapment efficiency (EE).** The entrapment efficiency of the DNLC was determined by the ultracentrifugation method. A volume of 5 mL of DNLCs was centrifuged (Hermle labortechnik GmbH, Germany) at 10,000 rpm for 30 min. The supernatant and pellet were collected; the pellet was dispersed with methanol.<sup>24</sup> The amount of drug present in the supernatant was determined by UV spectrophotometry using the following equation:

$$EE\% = \frac{W_i - W_f}{W_i} \times 100$$

where  $W_i$  is the amount of drug added initially and  $W_f$  is the amount of drug detected in the supernatant/pellet after centrifugation of the formulation

## 2.5 Preparation of a DNLC gel

A DNLC gel was prepared by mechanical stirring. Carbopol 934 was used as a gel-forming polymer; the required amount of carbopol was weighed and allowed to soak in a few mL of distilled water for 4 hours, after which it was placed under a mechanical stirrer.<sup>25</sup> Freshly prepared DNLC solution was added drop by drop into the beaker under con-

stant stirring, carefully observing to ensure uniform mixing of the polymer and DNLC dispersion. Propylparaben was added as a preservative, while triethanolamine was added to neutralize carbopol and to achieve topical consistency. Carbopol gels were prepared at two concentrations, 1% w/w and 1.5% w/w.

## 2.6 Characterization of gel formulations

**2.6.1 Homogeneity, grittiness, pH determination, and spreadability.** The prepared gels were tested for homogeneity by visual inspection after the gels had been set in the container. They were tested for their appearance and the presence of any aggregates. The prepared gels were evaluated microscopically for the presence of particles under a light microscope. pH was measured using a digital pH meter, which had been calibrated before the experiment. The bulb of the electrode was inserted into the gel, and the reading was noted. The experiment was performed in triplicate. To determine the spreadability, 1 g of the gel was placed on a horizontal glass plate, and a second glass plate was placed on the gel such that the gel was sandwiched between the glass plates. Then, a standard weight of 125 g was placed on top of the upper glass plate for 1 minute. The upper plate was then removed, and the diameter of the gel was measured.<sup>26</sup> The following formula was then used to calculate the spreadability:

$$S = d^2 \times \pi \div 4$$

where  $S$  is spreadability and  $d$  is the diameter of the gel in mm.

**2.6.2 Rheological evaluation.** Rheological evaluation was carried out on DNLC gels and NLC gels (NLCs without drug). The rheological properties were assessed using a Brookfield Rheocalc V32 rheometer (Brookfield, USA) equipped with a cone and plate geometry. Each sample was equilibrated at 28 °C before every measurement, and data analysis was done with the Brookfield rheocalc 2.010 application software. Viscosity vs. shear rate, as well as the viscoelastic modulus and phase angle vs. frequency, were also investigated, with measurements conducted in triplicate for each system.<sup>27</sup>

## 2.7 Drug content analysis of drug-loaded NLC Gels (DNLC gels)

0.5 g of the DNLC gel was accurately weighed and dissolved in 100 mL of pH 5.5 phosphate buffer solution in a volumetric flask. The volumetric flask was kept for 4 hours in an orbital shaker. The solution was then passed through filter paper and filtered. 1 mL of this solution was then taken into a 10 mL volumetric flask, and the final volume was made up with pH 5.5 phosphate buffer solution.<sup>28</sup> The absorbance was measured at 240 nm for clobetasol propionate and 224 nm for pramoxine hydrochloride. Phosphate buffer solution was used as a blank.

## 2.8 In vitro drug release from the DNLC gel

The release of CP and PH from DNLC gels was studied by the cellophane membrane method (Sigma Aldrich, India) at pH



5.5. Previously activated cellophane membrane was tied to one end of the open-ended tube, and 0.5 g of DNLC gel was placed into the tube through the other end.<sup>29</sup> The open-ended tube with the DNLC gel was suspended in the receptor compartment containing 30 mL of PBS–ethanol mixture (7:3) as release medium. This experimental setup was retained on a magnetic stirrer operating at 50 rpm and maintained at 37 °C. Sink condition was maintained throughout the experiment. At predetermined time intervals, samples were withdrawn from the receptor compartment and were replaced with an equal amount of fresh release medium. The amount of CP and PH in the release medium was determined using a UV-visible spectrophotometer set at 240 nm and 224 nm, respectively. The experiments were carried out in triplicate. Kinetic modeling of data was performed.

## 2.9 *Ex vivo* porcine skin studies

*Ex vivo* skin studies were conducted using porcine ear skin, which is considered a suitable model for permeation experiments. Pig ear skin was obtained from the local slaughterhouse and cleaned by washing with water. Hair present on the skin surface was removed using a scalpel blade. The underlying fatty layer was removed, and the skin was washed with normal saline and kept at –20 °C for further use.<sup>30</sup> The experiment was conducted on Franz diffusion cell apparatus; the surface area of skin exposed to the formulation was 2.54 cm<sup>2</sup>, and the receptor chamber was filled with 7 mL of PBS–ethanol mixture (7:3). The temperature was maintained at 32 °C, and the receptor chamber was stirred at 400 rpm.

**2.9.1 Skin permeation studies.** Skin samples were properly hydrated by soaking in pH 5.5 PBS for half an hour, then sandwiched between the donor and receptor compartments of the Franz diffusion cell. 0.5 g of the DNLC gel was applied to the skin on the donor side. At predetermined time intervals, samples were collected from the receptor compartment and replaced with equal amounts of buffer–ethanol mixture. The amounts of CP and PH permeated were measured using a UV-visible spectrophotometer set at 240 nm and 224 nm, respectively. The permeation experiment lasted 24 hours. The experiment was conducted in triplicate. The steady-state flux ( $J$ ) was calculated from the slope of the graph, and the permeability constant ( $P$ ) was determined using Fick's first law of diffusion. The enhancement ratio ( $E$ ) was calculated from the steady-state flux.<sup>30,31</sup>

**2.9.2 Drug retention studies.** The amount of drug retained in each layer of skin (stratum corneum, epidermis, and dermis) was determined. Skin samples were sandwiched between the donor and receptor compartments of the Franz diffusion cell apparatus. The skin samples were collected at predetermined time intervals and washed with PBS solution to remove the DNLC gel remaining on the skin surface. The dried skin samples were cut into 1 cm<sup>2</sup> pieces. Each piece was then fixed using tissue freezing medium and was cryo-sectioned with a microcryotome (Leica CM 1505 S) into stratum corneum (25 μm), epidermis (75 μm), and dermis (1 mm). CP and PH retained within the skin layers were extracted by incubating

the samples overnight in methanol in a shaking incubator at 37 °C, after which they were homogenized and centrifuged.<sup>30,31</sup> The amounts of CP and PH retained were determined using a UV-visible spectrophotometer set at 240 nm and 224 nm, respectively, and are expressed as μg cm<sup>-2</sup> of skin area.

**2.9.3 Dermal pharmacokinetic parameters.** The data obtained from *ex vivo* skin permeation studies were used to determine dermal pharmacokinetic parameters such as  $C_{\max}$ ,  $T_{\max}$ , AUC, AUMC, and MRT. These parameters were determined by using Phoenix WinNonlin® software.<sup>32</sup>

**2.9.4 Rhodamine-tagged DNLC gel skin retention study.** To determine the depth of penetration and retention of the DNLC in the formulation, a skin permeation experiment was conducted. The rhodamine-tagged DNLC gel was prepared by mixing rhodamine and DNLC gel on a magnetic stirrer overnight. 100 μL of rhodamine was mixed with 1 g of DNLC gel. The method used was the same as that of the previously explained permeation experiment, except that everything was performed in the dark to prevent the photolytic deactivation of rhodamine dye. After 24 h, skin samples were removed and cryosectioned. The cryosectioned skin samples were placed on poly-L-lysine (PLL)-coated glass slides, and fluorescence was detected using an Olympus-BX-51 fluorescent microscope.<sup>33</sup>

## 2.10 *In vivo* studies

*In vivo* animal studies were performed on male albino Wistar rats (250 g–300 g) for 28 days to evaluate the disease-mitigating property the DNLC gel formulation.

**2.10.1 Induction of atopic dermatitis in an animal model.** 2,4-Dinitrochlorobenzene (DNCB) was used to cause atopic dermatitis. Animals were anesthetized with isoflurane, their back hair was shaved, and 0.2 mL of DNCB in a 4:1 vehicle of acetone and olive oil was applied topically to a premarked 8 cm<sup>2</sup> region. Atopic dermatitis-like lesions formed following 4 administrations of DNCB with a 2 day gap between each treatment, the first two being sensitization (0.2 mL, 1% DNCB) and the last two being challenge (0.2 mL, 0.2% DNCB).<sup>34,35</sup>

**2.10.2 Atopic dermatitis studies.** The animals were divided into 7 groups ( $n = 6$ ). Group 1 was an untreated control; group 2: CP and PH-loaded NLC; group 3: conventional CP cream (0.05%); group 4: NLC gel treatment; group 5: CP NLC gel treatment; group 6: PH NLC gel treatment; and group 7: normal control. Each group, except the normal control, was induced with atopic dermatitis, while group 1 was not subjected to any treatment. Treatment for other groups was started on the 14<sup>th</sup> day after the disease was induced to a severe condition, and the treatment period was for 14 days. One fingertip dose of the formulation was applied evenly on the area premarked on the 14<sup>th</sup>, 17<sup>th</sup>, 21<sup>st</sup>, and 24<sup>th</sup> day. To retain the disease during the treatment period, once every 3 days, DNCB was administered. The animals were euthanized on the 28<sup>th</sup> day; the skin was collected and stored in 10% neutral phosphate-buffered formalin. Investigative global atopic dermatitis (IGAD) scoring was measured for each group every day by 3 individuals, among whom 1 was not made aware of the experiment to obtain an



unbiased blind scoring.<sup>36</sup> The area of atopic dermatitis disease induced was measured using ImageJ software.

**2.10.3 IgE and absolute eosinophil count (AEC).** Blood from the animals was collected from the retroorbital plexus on day 0, day 14, and day 28 to determine the amount of IgE and AEC in the plasma.<sup>37</sup>

**2.10.4 Histological analysis.** The skin samples collected at the end of euthanasia were treated with isopropanol and xylene and then embedded in paraffin. 5  $\mu\text{m}$  thick sections were cut using a microtome, stained with hematoxylin and eosin, mounted using DPX, and observed under an optical microscope equipped with a computer-controlled camera. The histological changes of all skin samples in comparison with the control animals were evaluated with the help of a veterinary pathologist, and the thickness of the epidermis was measured using Fiji Image J software.

### 2.11 Statistical analysis

The data were analyzed using the Student's *t*-test calculator, Graph Pad software, and QuickCalcs, and  $p < 0.05$  was considered to be significant.

## 3. Results and discussion

### 3.1 Characterization of DNLC

**3.1.1 Particle size and zeta potential.** Particle size is important in nanostructured carriers because it contributes to the interfacial area. Nanocarriers having a smaller particle size can easily penetrate into the deeper layers of skin, providing enhanced drug partitioning and adsorption. There is, however, no consensus in the literature on the exact size ranges of nano formulations.<sup>38</sup> The particle size and zeta potential of a DNLC were determined by the dynamic light scattering technique using a Zetasizer instrument. The average particle size and zeta potential were found to be  $66.95 \pm 5.27$  nm and  $-42.86 \pm 4.66$  mV, respectively, which were in accordance with our previous work (Dixit *et al.*).<sup>24</sup> This particle size can be attributed

to the technique adopted for the preparation of the DNLC, and also the increased concentration of surfactant aids in the reduction of particle size. The stability of the NLC dispersion can be represented by zeta potential. It is reported that a nano-dispersion with a zeta potential of  $< -60$  mV has excellent stability.<sup>39</sup> The DNLC exhibits a zeta potential of  $-42.86 \pm 4.66$  mV, possibly due to the usage of soya lecithin. The anionic components of lecithin may have contributed to the negative charge.<sup>40</sup> The polydispersity index (PDI) measures the size distribution of nanoparticles in the dispersion. Monodisperse samples with uniform particle size distributions have PDI values ranging from 0.1 to 0.7, whereas PDI values of more than 0.7 indicate that the dispersion has a broad size distribution. The prepared DNLC dispersion had a PDI value of 0.25, indicating that it is monodisperse, with uniform particle size.<sup>39</sup>

**3.1.2 SEM and TEM.** SEM and TEM studies were carried out to further determine the size and morphology of the DNLC. The measurement using the Zetasizer instrument does not involve measuring the actual size but only estimates the size of the NLC according to the light scattering pattern and intensity; hence, SEM and TEM analysis are useful.<sup>41</sup> The TEM result (Fig. 1A) reveals a particle having a size less than 120 nm. The SEM result (Fig. 1B) shows the NLC as aggregates, which could be the reason for the particle size between 100 nm to 150 nm. The aggregation might have occurred due to the sample preparation for SEM analysis.

**3.1.3 Entrapment efficiency.** Entrapment efficiency (EE) was calculated to determine the amount of CP and PH entrapped in the NLC. The average EE of CP and PH in the NLC was found to be  $75.47 \pm 3.26\%$  and  $87.75 \pm 2.14\%$ , respectively. These EE values could have been achieved due to the incorporation of drugs into the lipid phase, where the solid lipid was melted in the presence of liquid lipid. This caused disarray in the crystal order, causing imperfect lattice formation, which is a characteristic feature of NLCs that can help in the accommodation of drug molecules.<sup>42</sup> The EE value also depends on the nature of the drugs; CP and PH are both

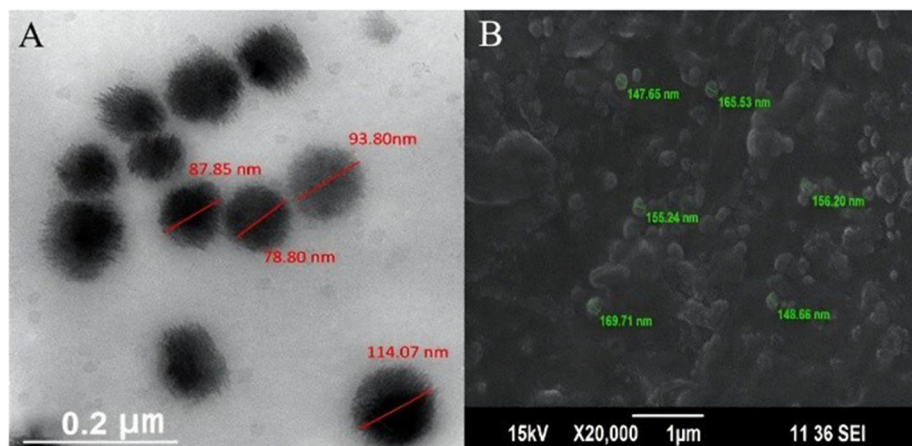


Fig. 1 TEM and SEM analysis: (A) TEM image; (B) SEM image.



lipophilic drugs. The use of soya lecithin in the preparation of the DNLC also influences the entrapment of drugs. It is reported that lecithin reduces the possibility of drug loss and provides more space for the drug.<sup>43</sup>

### 3.2 Preparation of the DNLC gel

DNLC dispersions lack the consistency required for topical use; thus, the DNLC must be incorporated into a carrier to give a suitable form for topical treatment.<sup>44</sup> Carbopol gel acts as a secondary carrier for medicines and a medium for DNLCs. Carbopol gels are suitable for nanoparticle inclusion,<sup>45</sup> allowing the NLC to permeate the skin during a longer contact duration. Soaking in carbopol makes it smooth and viscous, and mechanical stirring loosens the polymer chains. Triethanolamine neutralizes carbomer, allowing it to thicken to the desired consistency for topical application. Table 1 shows the formula for making the gel.

### 3.3 Characterization of gel formulations

**3.3.1 Homogeneity, grittiness, pH determination, and spreadability.** Physicochemical properties such as homogeneity, grittiness, pH, and spreadability of the DNLC gel and plain gel were studied, and the results are presented in Table 2. It was observed that all the gel formulations were homogeneous without the presence of any gritty particles and exhibited a pH range of 5.8 to 6.2, which falls within the physiologically acceptable range for skin application. This pH range helps maintain

the natural acidic mantle of the skin and minimizes the risk of irritation.<sup>46</sup> As the gel strength increases, the spreadability decreases, which can be seen in Table 3. The addition of the DNLC further increased the spreadability, which is due to the lipid nature of the DNLC dispersion.

**3.3.2 Rheological evaluation.** Rheological evaluation is essential to determine the flow properties of the system since it is intended for topical application. The plot of elastic modulus ( $G'$ ), viscous modulus ( $G''$ ), and phase angle vs. frequency (Fig. 2A) has revealed that  $G'$  is greater than  $G''$  ( $G' > G''$ ), which is ideal for a topical gel. The value of the phase angle being less than  $10^\circ$  is indicative of the formulation having gel-like behavior and not flowing unless a shear force is applied.<sup>47,48</sup> The plot of viscosity vs. shear rate (Fig. 2B) revealed that the gel formulations (DNLC gel and plain gel) exhibit shear-thinning behavior, characterized by a decrease in viscosity of the formulation as the shear rate increases. The shear-thinning behavior is considered essential for topical gels to be extruded easily from the container.

### 3.4 Drug content analysis of DNLC gels

It is essential to determine the amount of CP and PH present in one fingertip unit of gel (*i.e.*, 0.5 g of DNLC gel) because *in vitro* drug release studies, *ex vivo* skin studies, and *in vivo* studies require knowledge of the drug content in each application. It was found that  $0.221 \pm 0.012$  mg of CP and  $4.670 \pm 0.093$  mg of PH were present in one fingertip unit of gel (*i.e.*, 0.5 g).

### 3.5 *In vitro* drug release from the DNLC gel

*In vitro* drug release from the DNLC gel was assessed using the dialysis membrane method at  $37^\circ\text{C}$  and 50 rpm. The drug release pattern from the DNLC gel is shown in Fig. 3. A biphasic release pattern was observed for CP, with an initial burst release followed by a sustained release, while PH showed a sustained release pattern. 33% of the CP and 3% of the PH were released within the first hour; by the end of 24 h, 84% of the CP and 64% of the PH were released. The initial burst release of CP may be due to the localization of CP in the outer shell of

**Table 1** Design for preparing NLC gel and DNLC gel formulations

Sl. no	Ingredients			
	Carbopol 934 (% w/w)	Propyl paraben (% w/w)	DNLC (mL)	Distilled water (mL)
1	1	0.002	50	—
2	1.5	0.002	50	—
3	1	0.002	—	50
4	1.5	0.002	—	50

**Table 2** Homogeneity, grittiness, color, spreadability, and pH of NLC gel and DNLC gel formulations

Sl. no	Gel type	Homogeneity	Grittiness	Color	Spreadability ( $\text{mm}^2$ )	pH
1	1% w/w NLC gel	+++	—	Transparent	2109.1	$5.81 \pm 0.31$
2	1.5% w/w NLC gel	+++	—	Transparent	1950.0	$6.12 \pm 0.12$
3	1% w/w DNLC gel	+++	—	Color	2446.1	$5.92 \pm 0.04$
4	1.5% w/w DNLC gel	+++	—	Color	2359.5	$6.01 \pm 0.14$

**Table 3** Permeation parameters from an *ex vivo* porcine skin permeation study

Sample	Steady state flux ( $\mu\text{g cm}^{-2} \text{h}^{-1}$ )	Enhancement ratio	Permeability constant ( $\text{cm}^2 \text{h}^{-1}$ )
Clobetasol drug solution	3.0713	—	$0.01288 \pm 0.003$
Pramoxine drug solution	5.9001	—	$0.00118 \pm 0.001$
Clobetasol from DNLC gel	5.8862	1.92	$0.024 \pm 0.002$
Pramoxine from DNLC gel	9.5295	1.62	$0.002 \pm 0.001$
Clobetasol from the marketed ointment	4.1213	—	0.0169



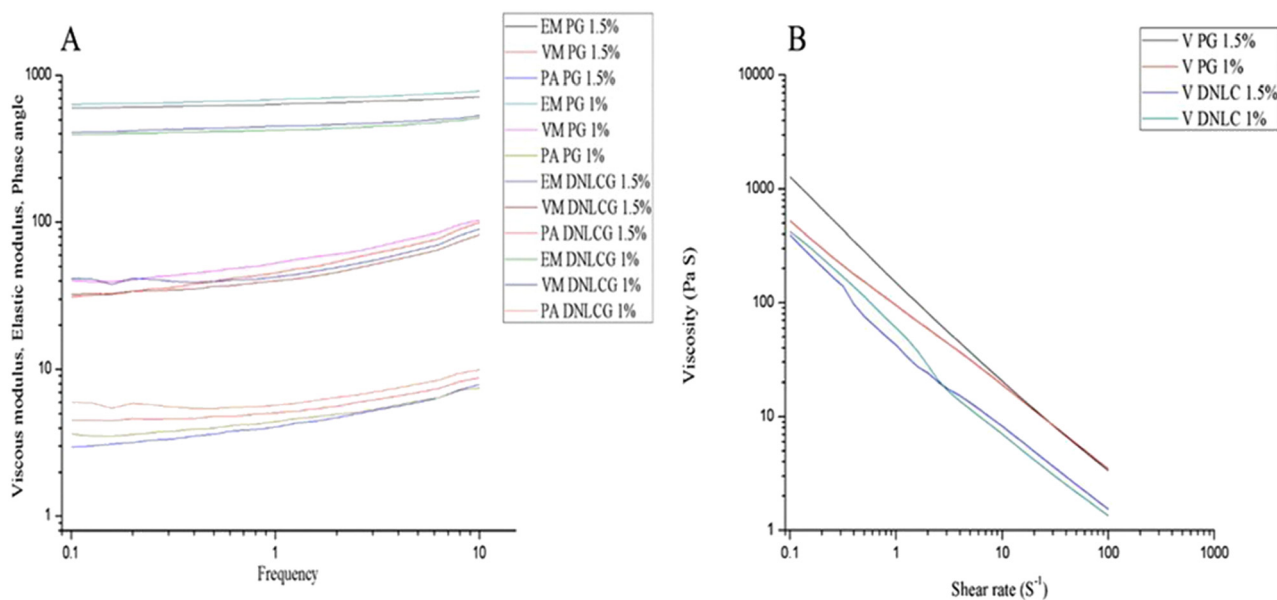


Fig. 2 Rheological evaluation of plain gel (PG) and DNLC gel (DNLCG): (A) elastic modulus (EM), viscous modulus (VM), and phase angle (PA) vs frequency. (B) Viscosity (V) vs. Shear rate.

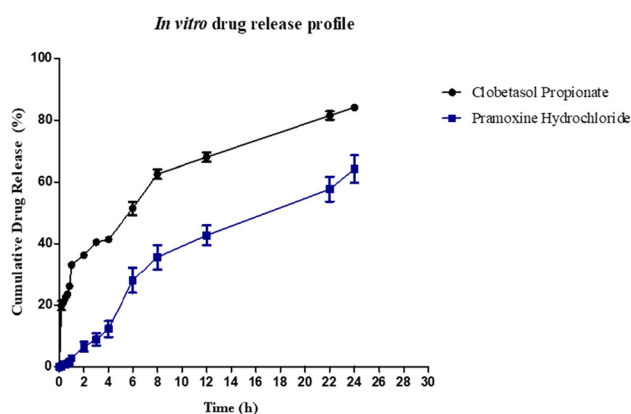


Fig. 3 *In vitro* drug release profile ( $n = 3$ ).

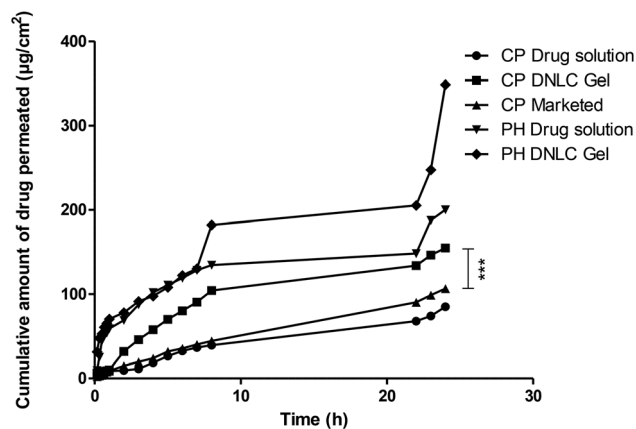


Fig. 4 *Ex vivo* skin permeation studies ( $n = 3$ ).

the NLC, while untrapped drug in the NLC dispersion could have been dispersed in the gel matrix, which could have caused the initial burst release.<sup>49</sup> A sustained-release pattern was observed in the case of PH, which may be due to the localization of PH in the core of the NLC. The release kinetics of drugs from the formulation was determined by fitting the *in vitro* drug release data into zero order, first order, Higuchi, and Korsmeyer–Peppas models. The release of CP can be best fitted to first-order kinetics, while the release of PH can be best fitted to zero-order kinetics; the Korsmeyer–Peppas model was used to determine the release mechanism, and it was seen that CP followed Fickian diffusion, while PH followed super case II.

### 3.6 *Ex vivo* drug permeation studies

*Ex vivo* skin permeation studies were carried out to determine the amount of drug that permeated across the skin from the

DNLC gel, and the results were compared with those of marketed CP cream and CP drug solution. The results (Fig. 4) revealed that drugs from the DNLC gel showed better skin permeation when compared with individual drug solutions, and permeation of CP from the DNLC gel was enhanced 1.42 times when compared with permeation from the marketed CP cream. Table 3 lists the steady-state flux, enhancement ratio, and permeability coefficient of the formulations. CP from the DNLC showed a permeability flux of  $5.88 \mu\text{g cm}^{-2} \text{h}^{-1}$  and an enhancement ratio of 1.92 when compared with that of the CP drug solution, whereas the PH from the DNLC gel showed a permeability flux of  $9.52 \mu\text{g cm}^{-2} \text{h}^{-1}$  and an enhancement ratio of 1.62 when compared with that of the PH drug solution. This enhancement of drug permeation from the DNLC gel may be due to the incorporation of drugs into NLC particles in the nanometric size range that can penetrate the skin, forming



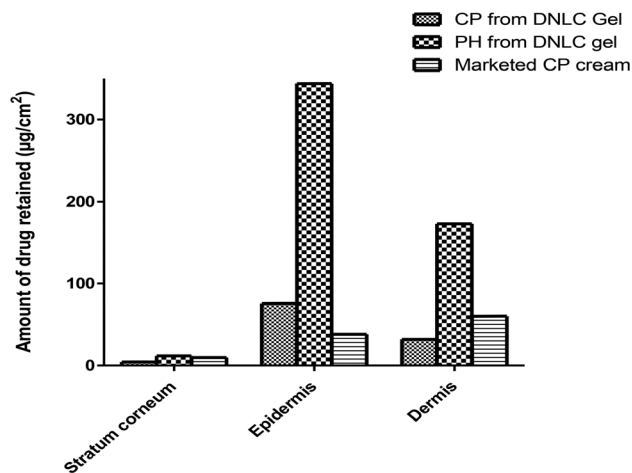


Fig. 5 Drug retention study at the end of 24 h in the stratum corneum, epidermis, and dermis.

micro-drug reservoirs in dermal layers by enhancing the permeation, which is seen from the increase in the enhancement ratio. The steady-state flux ( $J_{ss}$ ) was obtained from the slope of

the plot using a linear regression analysis. The permeability coefficient ( $K_p$ ) of the drug through the membrane was calculated using the following equation:

$$K_p = \frac{J_{ss}}{C}$$

where  $C$  is the initial concentration of the drug in the donor compartment.

The penetration-enhancing effect was calculated in terms of the enhancement ratio (ER):

$$ER = \frac{J_{ss}F}{J_{ss}C}$$

where,  $J_{ss}F$  is  $J_{ss}$  of the formulation and  $J_{ss}C$  is  $J_{ss}$  of the control

### 3.7 *Ex vivo* drug retention studies

*Ex vivo* drug retention studies were carried out to determine the amount of drug retained in different layers of skin at the end of the 24<sup>th</sup> hour. The amounts of CP retained at the end of 24 h (Fig. 5) in stratum corneum, epidermis and dermis were  $4.25 \pm 0.02 \mu\text{g}$ ,  $75.77 \pm 0.01 \mu\text{g}$  and  $32.04 \pm 0.012 \mu\text{g}$ , respectively, while the amounts of PH retained at the end of 24 h in stratum

Table 4 Pharmacokinetic parameters

Pharmacokinetic parameters	Pramoxine hydrochloride			Clobetasol propionate		
	SC	Epidermis	Dermis	SC	Epidermis	Dermis
$T_{max}$ (h)	2	24	24	2	24	24
$C_{max}$ (µg)	99.86	344.01	172.85	17.77	75.77	32.04
AUC last (h µg L <sup>-1</sup> )	141.84	4128	2074.2	51	909.24	384.48
MRT last	7.31	17.08	13.99	8.41	15.73	15.03

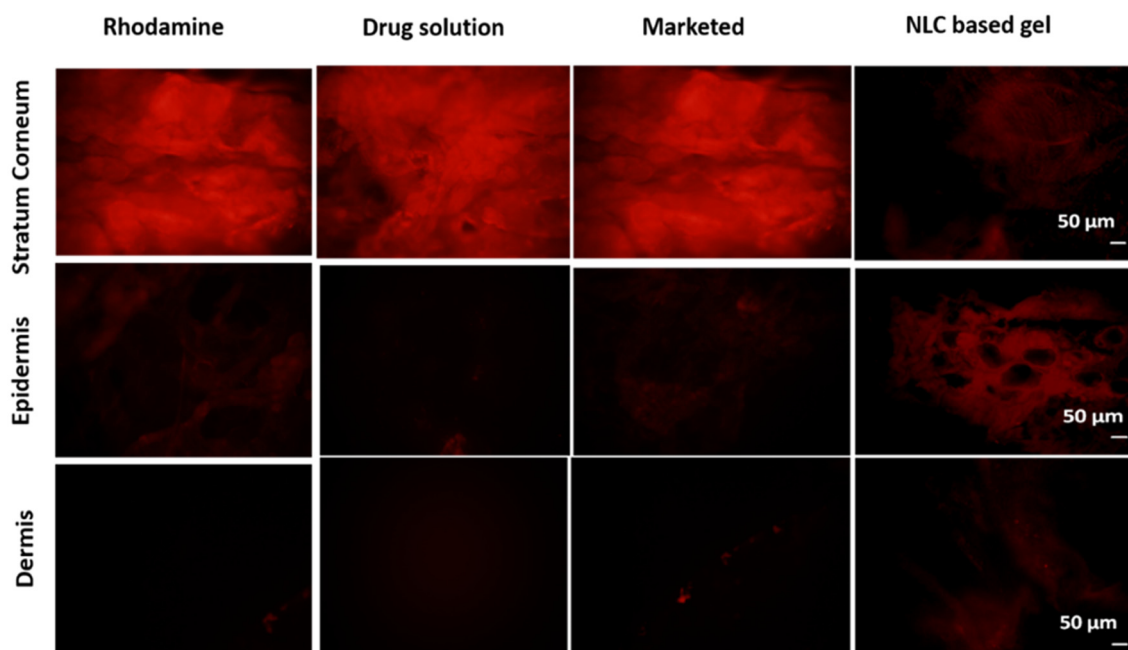


Fig. 6 Rhodamine-tagged fluorescence images.



corneum, epidermis and dermis were  $11.82 \pm 0.003 \mu\text{g}$ ,  $344.0 \pm 0.05 \mu\text{g}$  and  $172.85 \pm 0.040 \mu\text{g}$ , respectively. It is plausible that increased PH retention would prolong its numbing effect, thereby reducing itch and improving patient comfort. It can be seen that a greater amount of CP is retained from the DNLC gel compared to the marketed CP cream, which could be due to the incorporation of CP into the nanocarrier, enabling drug retention. More of the drug is retained in the epidermal and dermal region that constitutes the dermoepidermal junction.

### 3.8 Dermal pharmacokinetic parameters

The data obtained from *ex vivo* porcine skin studies were used to determine various dermal pharmacokinetic parameters,

including  $C_{\text{max}}$ ,  $T_{\text{max}}$ , AUC, AUMC, and MRT, which are presented in Table 4.

### 3.9 Rhodamine-tagged DNLC gel skin retention study

A skin retention study using rhodamine-tagged DNLC gel was carried out to confirm the skin penetration and retentive properties of the DNLC. The investigation was conducted over 24 hours using Franz diffusion cell apparatus; throughout the experiment, the system was kept out of direct sunlight to prevent photolytic breakdown of rhodamine. Fig. 6 shows various fluorescence pictures that reveal how the rhodamine-tagged DNLC-treated skin samples fluoresced; the rhodamine-tagged commercial CP cream and medication solution did not

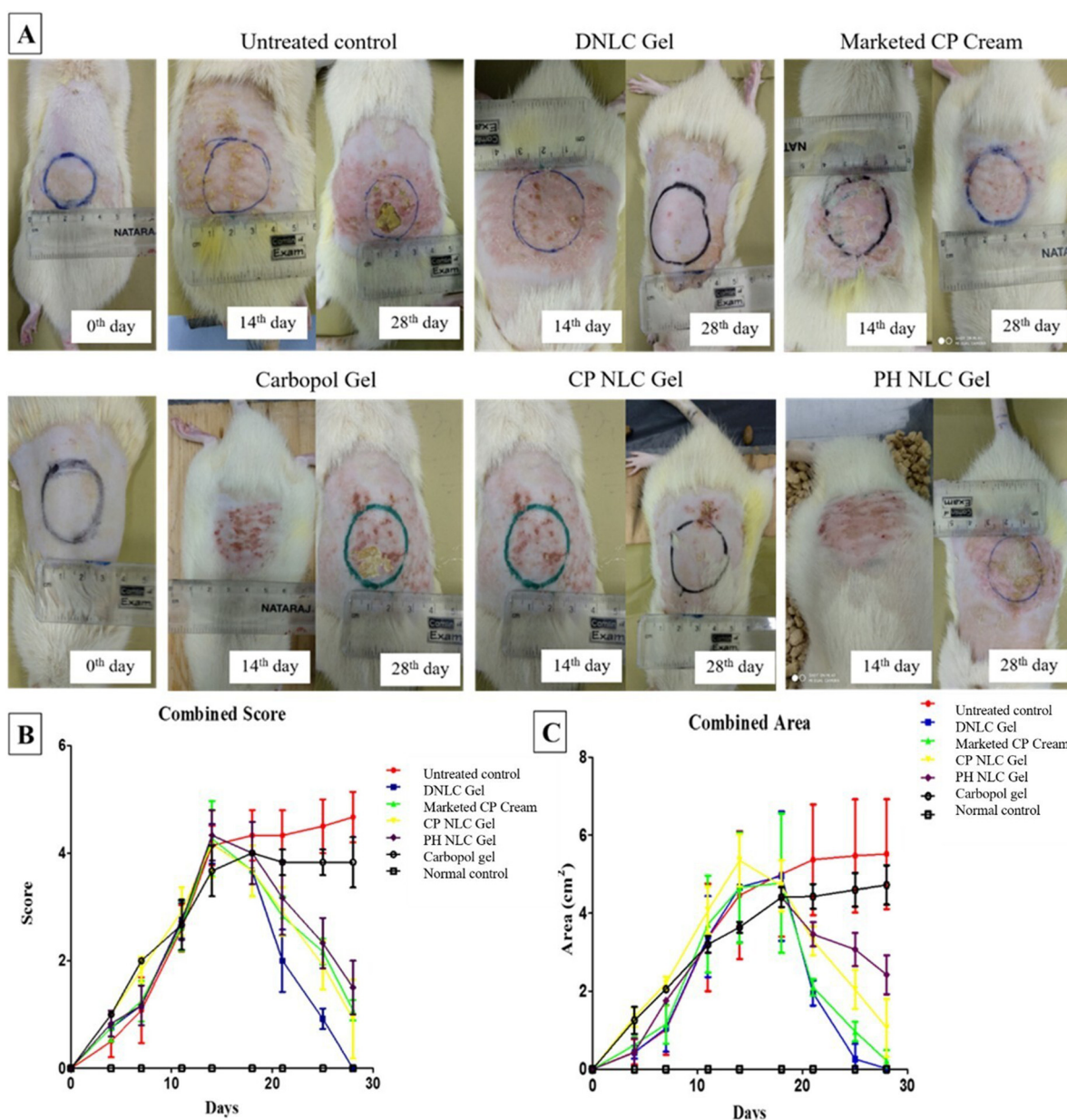


Fig. 7 *In vivo* animal studies ( $n = 6$ ). (A) 0th day, 14th day, and 28th day images of the animal. (B) IGAD score. (C) Area of the induced disease.



fluoresce in the epidermis or dermal region. This experiment further demonstrates the capacity of the DNLC to penetrate and persist in dermal layers.

### 3.10 *In vivo* animal studies

#### 3.10.1 Induction of atopic dermatitis in an animal model.

Atopic dermatitis-type skin lesions were induced on rat back skin by the topical application of 2,4 DNCB. Many investigators have used murine models to carry out *in vivo* studies on atopic dermatitis, where these models are of two types: (a) spontaneous mutants and genetically engineered mutants such as NC/Nga rat and IL-4/18-overexpressing rat; (b) sensitizer-induced models

(using ovalbumin, microbial antigen, and chemical reagents like picryl chloride, *i.e.* 2,4,6-trinitrochlorobenzene, or 2,4 dinitrochlorobenzene).<sup>50,51</sup> Among these, the murine models with repeated sensitizer application possess benefits in reproducibility in atopic dermatitis-like features.<sup>52,53</sup> Upon repeated topical application of DNCB on the skin, an immune response conversion from a Th<sub>1</sub> to Th<sub>2</sub>-mediated reaction, along with high serum IgE levels, epidermal hyperplasia, and infiltration of mast cells in dermis, was seen, which are all regarded as particular features of human atopic dermatitis.<sup>53,54</sup> Hence, to create an animal model, atopic dermatitis was induced in Wistar rats using 2,4-dinitrochlorobenzene as a sensitizer.

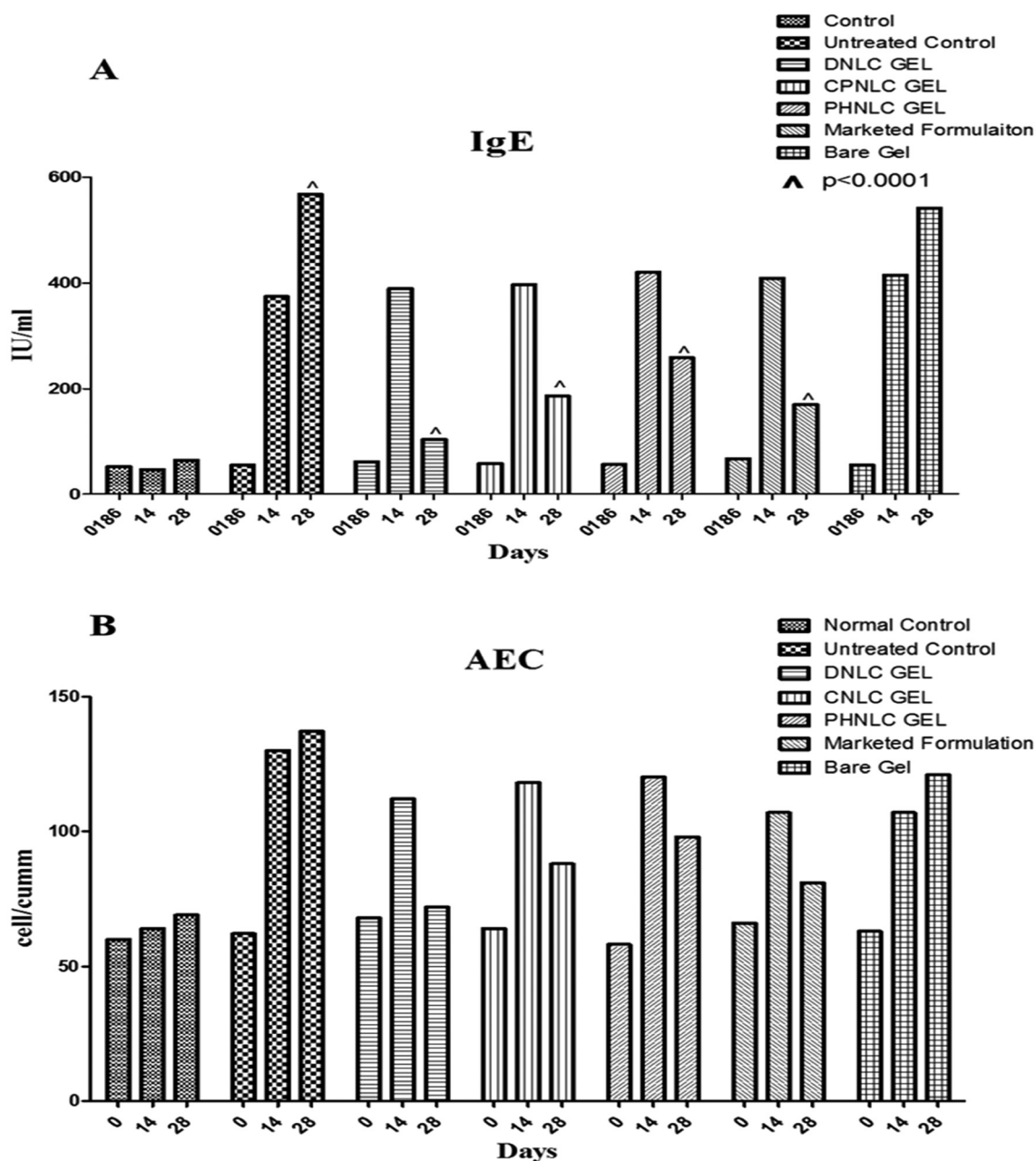


Fig. 8 IgE and AEC serum levels at the 0th day, 14th day, and 28th day. (A) IgE ( $p < 0.0001$ ); (B) AEC.



**3.10.2 Atopic dermatitis animal studies.** The animals were divided into seven groups ( $n = 6$ ). Group 1 was the untreated control in which the animals were induced with disease but were not treated; group 2 was combinational therapy in which after the induction of disease the animals were treated with CP and PH-loaded NLC gel; group 3 was conventional therapy in which after the induction of disease, the animals were treated with marketed CP cream (0.05% CP); group 4 was plain gel treatment in which the animals were treated with plain NLC gel after the induction of disease; group 5, anti-inflammatory therapy in which the animals, after disease induction, were treated with CP-loaded NLC gel (0.05%); group 6 was anti-pruritic therapy in which the animals were treated with PH NLC gel; and group 7 was the normal control in which the animals were not induced with disease. Fig. 7(A) shows the images of animal studies at days 14 and 28, Fig. 7(B) shows the atopic dermatitis score of all the groups, and Fig. 7(C) shows the area of disease induced. From the *in vivo* animal studies, it

was seen that the prepared CP and PH-loaded NLC gels decreased the induced disease on a par with that of the marketed CP cream, which can be seen from Fig. 7; the IGAD score and area decreased after the beginning of the treatment and attained 0 by the end of the 28<sup>th</sup> day, whereas the untreated control group retained the disease throughout the study period. Group 4, which involved plain gel therapy, showed no reduction in disease due to the absence of drug, whereas group 5, which employed anti-inflammatory therapy, demonstrated a reduction in disease, albeit slightly less than that achieved with conventional therapy. Group 6 also showed a reduction in IGAD score, but the area of disease induced was not decreased sufficiently, which could be due to the absence of CP, which mainly reduces inflammation and atopic dermatitis-like lesions.

**3.10.3 Serum IgE and AEC count.** The blood collected during the *in vivo* animal studies was evaluated for levels of serum IgE and AEC. Generally, IgE and AEC levels are elevated

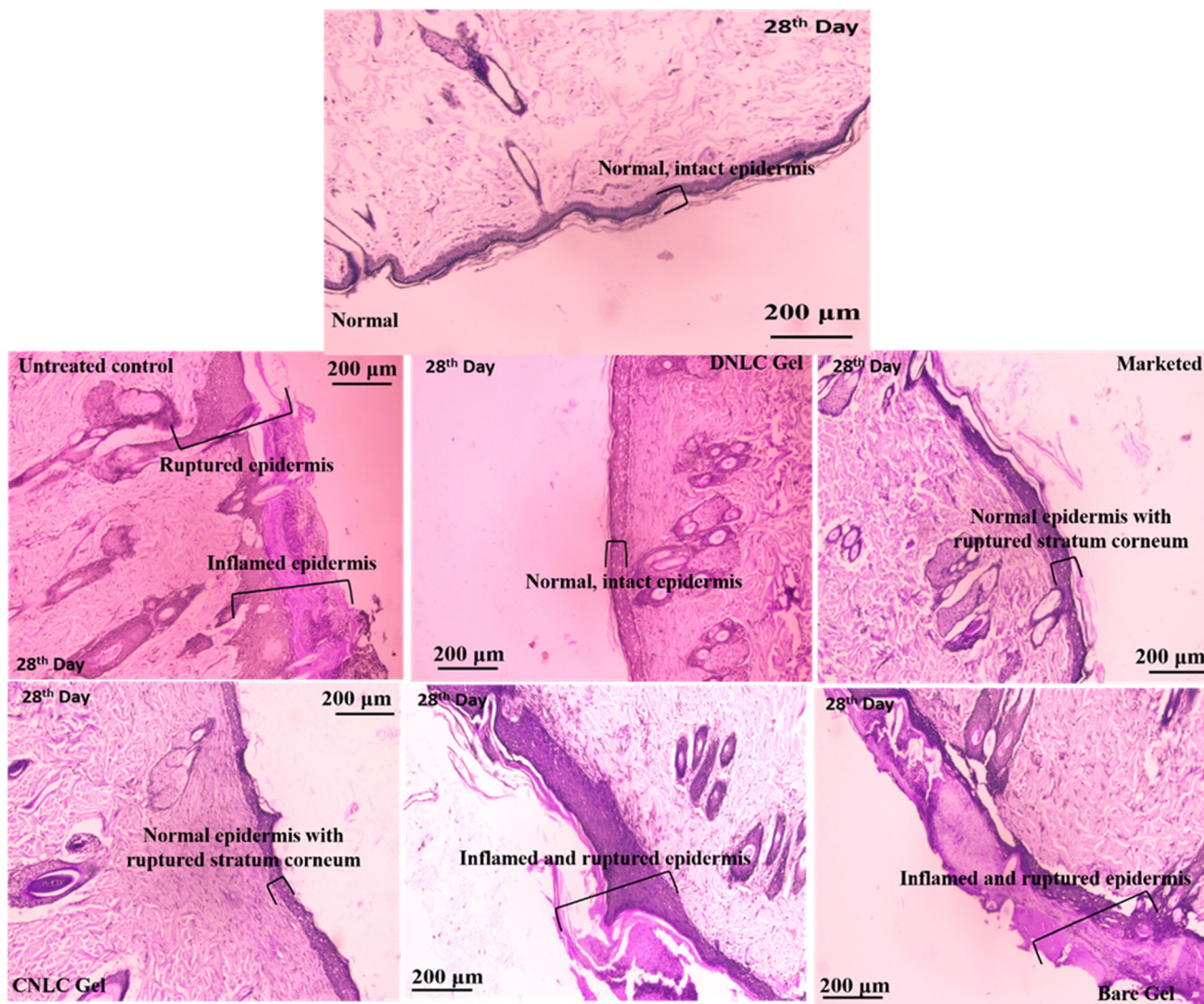


Fig. 9 Histological evaluation of skin sections after the 28th day.



in the blood of patients with atopic dermatitis; hence, it is essential to determine the levels of IgE and AEC. Blood samples were collected from the retroorbital plexus of rats at 3 time points in the study, which are on the 0<sup>th</sup> day, which is the day before the topical application of DNCB, which gives the value of IgE and AEC before induction of disease; on the 14<sup>th</sup> day, which is the day before beginning treatment and gives the value of IgE and AEC after the induction of disease; and on the 28<sup>th</sup> day, which is the day of euthanasia giving the values of IgE and AEC after the treatment of disease. Fig. 8(A) presents the values of IgE, and Fig. 8(B) presents the values of AEC. It can be seen that the values of IgE and AEC are low for the normal control animal group; in the disease control group, the values of IgE and AEC are significantly elevated, among the treatment groups. The DNLC gel treatment group showed the best reduction in IgE and AEC values, followed by the marketed CP cream. This could be due to the presence of CP in both formulations, which helps reduce inflammation. CPNLC gel treatment and PHNLC gel treatment groups also showed a reduction in IgE and AEC values, whereas bare gel, *i.e.*, the plain NLC gel-treated group, showed no reduction in the values of IgE and AEC.

**3.10.4 Histological analysis.** After euthanasia, skin samples were removed, and histological sections were evaluated (Fig. 9). From the histological sections, the thickness of the epidermis was measured using ImageJ software (Fig. 10). The skin histological studies revealed the increased epidermal thickness (acanthosis) along with focally fused pitted ridges, spongiosis, neutrophilic abscess, and areas of ulceration in the untreated control group, showing an epidermal thickness of  $354.32 \pm 63.71 \mu\text{m}$ . The normal control group showed an epidermal thickness of  $54.13 \pm 3.34 \mu\text{m}$  with normal epidermis, dermis, and dermal appendages. The DNLC therapy animal group showed normal epidermis, overlying dermis and

dermal appendages with an epidermal thickness of  $60.49 \pm 10.24 \mu\text{m}$ , which was close to that of the normal control group indicating that treatment with the DNLC gel has significantly reduced the induced disease, while the conventional therapy (marketed) group showed similar histological features with the epidermal thickness found to be  $86.4 \pm 12.66 \mu\text{m}$ . The anti-inflammatory group showed an epidermal thickness of  $74.69 \pm 14.73 \mu\text{m}$ . The plain gel treatment showed epidermis with irregular acanthosis and ulcerations with an epidermal thickness of  $316.50 \pm 55.61 \mu\text{m}$ , in which the disease was not reduced. Treatment with the DNLC gel helped maintain normal dermal features of the skin, which resemble those of the normal control group. Disease control and bare gel (NLC gel without drugs) showed ruptured and inflamed epidermis, and the epidermal thickness was also high.

## 4. Conclusion

DNLCs were prepared using the optimized formula from our previous work, and DLS and TEM analyses confirmed the nanoparticle size range, consistent with prior findings. This study primarily focused on loading DNLCs into a topical gel system to evaluate their effectiveness in mitigating disease by improving skin permeation and retention. The DNLC gel was successfully prepared; rheological evaluation confirmed it exhibited a shear-thinning behavior. *In vitro* drug release studies showed an initial burst followed by a sustained release pattern. *Ex vivo* skin studies using porcine inner ear skin, chosen for its morphological similarity to human skin, demonstrated that drugs from DNLC gels permeated the skin better than commercial creams, with enhanced drug retention when loaded into NLCs. Rhodamine-tagged DNLC gel retention fluorescence studies suggested that NLCs can form micro-drug reservoirs in the skin, enabling controlled drug release. *In vivo* animal studies confirmed that the DNLC gel is more effective in treating atopic dermatitis than commercial creams or individual drug-loaded DNLC gels, attributed to the sequential and distinct pharmacological actions of CP and PH. Further studies will include pharmacodynamic interaction assays to understand the nature of drug combinations within the DNLC system, and clinical studies in humans to confirm its efficacy. In conclusion, clobetasol propionate- and pramoxine hydrochloride-loaded NLC gels demonstrate improved skin retention and permeation, supporting their potential in effectively managing atopic dermatitis.

## Conflicts of interest

The authors have no conflict of interest.

## Ethical statement

All animal procedures were approved by the Institutional Animal Ethical Committee of Amrita Institute of Medical Sciences (AIMS) and conducted in accordance with the guide-

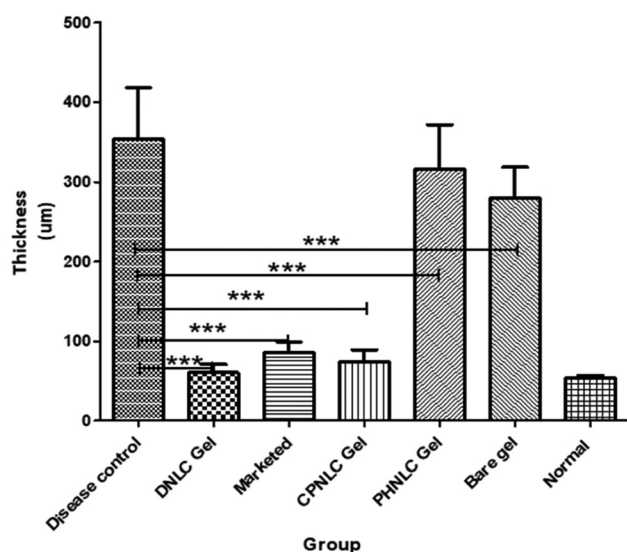


Fig. 10 Epidermal thickness calculated from the histological sections ( $n = 6$ ).



lines of the Committee for the Control and Supervision of Experiments on Animals (CPCSEA), Government of India.

## Data availability

The data supporting this article have been included as part of the ESI.†

## Acknowledgements

The authors would like to acknowledge the Amrita Center for Nano Sciences and Molecular Medicine, STIC CUSAT, and the Central Animal House Facility for graciously helping in conducting this research work.

## References

- 1 S. Nutten, Atopic Dermatitis: Global epidemiology and risk factors, *Ann. Nutr. Metab.*, 2015, **1**, 8–16.
- 2 M. Asher, *et al.*, Worldwide time trends in the prevalence of symptoms of asthma, allergic rhinoconjunctivitis, and eczema in childhood: ISAAC phases one and three repeat multicountry cross-sectional surveys, *Lancet*, 2006, **368**, 733–743.
- 3 S. J. Brown and W. H. McLean, One remarkable molecule: filaggrin, *J. Invest. Dermatol.*, 2012, **132**(32), 751–762.
- 4 J. M. Spergel and A. S. Paller, Atopic dermatitis and the atopic march, *J. Allergy Clin. Immunol.*, 2003, **112**, S118–S127.
- 5 D. Y. M. Leung, Atopic dermatitis: new insights and opportunities for therapeutic interventions, *J. Allergy Clin. Immunol.*, 2000, **105**, 860–876.
- 6 C. M. Keck, *et al.*, A new concept for the treatment of atopic dermatitis: Silver-nanolipid complex (sNLC), *Int. J. Pharm.*, 2014, **462**, 44–51.
- 7 K. P. Hetal, *et al.*, Topical delivery of clobetasol propionate loaded micro emulsion based gel for effective treatment of vitiligo: Ex vivo permeation and skin irritation studies, *Colloids Surf.*, 2013, **102**, 86–94.
- 8 I. Ozacan, *et al.*, Enhanced delivery of diflucortolone valerate using lecithin/chitosan nanoparticles: *in vitro* and *in vivo* evaluations, *Int. J. Nanomed.*, 2013, **8**, 461–475.
- 9 B. Ulya, *et al.*, Microparticulate based topical delivery system of clobetasol propionate, *AAPS PharmSciTech*, 2011, **3**, 949–957.
- 10 C. McCuaig, The itch that rashes: an update on atopic dermatitis, *Can. J. Diagn.*, 2003, **20**, 69–76.
- 11 B. Pfeifer-Ott and J. Godfrey, Patients report many different signs and symptoms as indicators of impending flare in atopic eczema, *J. Eur. Acad. Dermatol. Venereol.*, 2003, **17**(3), 181.
- 12 D. Fivenson, *et al.*, The effect of atopic dermatitis on total burden of illness and quality of life on adults and children in a large managed care organization, *J. Manag. Care Pharm.*, 2002, **8**, 333–342.
- 13 P. Warschburger, *et al.*, Psychological adjustments in parents of young children with atopic dermatitis: which factors predict parental quality of life in German and Ugandan patients, *Br. J. Dermatol.*, 2001, **144**, 305–309.
- 14 C. G. Burkhart and H. R. Burkhart, Contact irritant dermatitis and anti-pruritic agents: the need to address the itch, *J. Drugs Dermatol.*, 2003, **2**(2), 143–146.
- 15 T. A. Young, *et al.*, A pramoxine-based anti-itch lotion is more effective than a control lotion for the treatment of uremic pruritus in adult hemodialysis patients, *J. Dermatol. Treat.*, 2009, **20**(2), 76–81.
- 16 R. R. Gupta, *et al.*, AOT water-in-oil microemulsions as a penetration enhancer in transdermal drug delivery of 5-fluorouracil, *Colloids Surf., B*, 2005, **41**(1), 25–32.
- 17 A. Luis, *et al.*, *In vitro* skin penetration of clobetasol from lipid nanoparticles: drug extraction and quantification in different skin layers, *Braz. J. Pharm. Sci.*, 2012, **4**, 811–817.
- 18 I. Jawaid, *et al.*, Photochemistry of clobetasol propionate, a steroidal anti-inflammatory drug, *Arxivoc*, 2006, **11**, 91–98.
- 19 J. Garg, K. Pathania, S. P. Sah and S. V. Pawar, Nanostructured lipid carriers: a promising drug carrier for targeting brain tumours, *Future J. Pharm. Sci.*, 2022, **8**(1), 25.
- 20 E. B. Souto, *et al.*, Development of a controlled release formulation based on SLN and NLC for topical clotrimazole delivery, *Int. J. Pharm.*, 2004, **271**(1), 71–77.
- 21 M. Radtke, *et al.*, Nanostructured lipid carriers: a novel generation of solid lipid drug carriers, *Pharm. Technol. Eur.*, 2005, **17**(4), 45–50.
- 22 S. Tiwari, *et al.*, SLNs based on co-processed lipids for topical delivery of terbinafine hydrochloride, *J. Pharm. Drug Dev.*, 2014, **1**(6), 604.
- 23 S. Nikoli, *et al.*, Skin photoprotection improvement: synergistic interaction between lipid nanoparticles and organic UV filters, *Int. J. Pharm.*, 2011, **414**(1–2), 276–284.
- 24 C. M. Dixit, *et al.*, Development and *in vitro* evaluation of nanolipid carrier of clobetasol propionate and pramoxine hydrochloride for topical delivery, *Int. J. App. Pharm.*, 2018, **10**(3), 28–36.
- 25 H. Fei, *et al.*, Nanostructured lipid carriers (NLC) based topical gel of flurbiprofen: Design, characterization and *in vivo* evaluation, *Int. J. Pharm.*, 2012, **439**, 349–357.
- 26 L. Panigrahi, *et al.*, Formulation and Evaluation of Lincomycin HCl Gels, *Ind. J. Pharm. Sci.*, 1997, **59**(6), 330–332.
- 27 N. Margaret, *et al.*, Modern ointment base technology Comparative evaluation of bases, *J. Am. Pharm. Assoc.*, 1956, **4**, 212–217.
- 28 R. Khullar, *et al.*, Emulgels: a surrogate approach for topically used hydrophobic drugs, *Int. J. Pharma BioSci.*, 2011, **1**, 117–128.
- 29 K. Yadhu, *et al.*, Enhanced lymphatic uptake of leflunomide loaded nanolipid carrier via chylomicron formation for the treatment of rheumatoid arthritis, *Adv. Pharm. Bull.*, 2018, **8**(2), 257–265.



- 30 P. Rajitha, *et al.*, Comparative anti-psoriatic efficacy studies of clobetasol loaded chitin nanogel and marketed cream, *Eur. J. Pharm. Sci.*, 2017, **96**, 193–206.
- 31 M. Sabitha, *et al.*, Curcumin loaded chitin nanogels for skin cancer treatment via the transdermal route, *Nanoscale*, 2012, **1**, 239–250.
- 32 E. Mohammed, *et al.*, Atorvastatin-loaded nanostructured lipid carriers (NLCs): strategy to overcome oral delivery drawbacks, *Drug Delivery*, 2017, **24**(1), 932–941.
- 33 G. Divya, *et al.*, Acitretin and aloe-emodin loaded chitin nanogel for the treatment of psoriasis, *Eur. J. Pharm. Biopharm.*, 2016, **107**, 97–109.
- 34 Y. Fujii, *et al.*, Characterization of 2,4-dinitrochlorobenzene-induced chronic dermatitis model in rats, *Skin Pharmacol. Physiol.*, 2009, **22**(5), 240–247.
- 35 K.-S. Lee, *et al.*, A novel model for human atopic dermatitis: Application of repeated DNCB patch in BALB/c mice, in comparison with NC/Nga mice, *Lab. Anim. Res.*, 2010, **26**(1), 95–102.
- 36 Y. M. L. Donald, *et al.*, Thymopentin therapy reduced the clinical severity of atopic dermatitis, *J. Allergy Clin. Immunol.*, 1990, **85**(5), 927–933.
- 37 M. Masahiro, *et al.*, IgE hyperproduction through enhanced tyrosine phosphorylation of janus kinase 3 in NC/Nga mice, a model for human atopic dermatitis, *J. Immunol.*, 1990, **162**, 1056–1063.
- 38 J. Liu, *et al.*, Isotretinoin-loaded solid lipid nanoparticles with skin targeting for topical delivery, *Int. J. Pharm.*, 2007, **328**(2), 191–195.
- 39 R. H. Muller, *et al.*, Solid lipid nanoparticles (SLN) for controlled drug delivery – a review of the state of the art, *Eur. J. Pharm. Biopharm.*, 2000, **50**(1), 161–177.
- 40 Q. Xu, *et al.*, Soyabean based surfactants and their applications, in *Soyabean application and technology*, 2011, vol. 20, pp. 341–362.
- 41 K. Raza, *et al.*, Lipid-based capsaicin-loaded nano-colloidal biocompatible topical carriers with enhanced analgesic potential and decreased dermal irritation, *J. Liposome Res.*, 2014, **24**(4), 290–296.
- 42 D. Patel, *et al.*, Nanostructured lipid carriers (NLC) based gel for the topical delivery of aceclofenac: Preparation, characterization and *in vivo* evaluation, *Sci. Pharm.*, 2012, **80**, 749–764.
- 43 Q. F. Hu, *et al.*, Preparation and characterization of steric acid nanostructured lipid carriers by solvent diffusion method in an aqueous system, *Colloids Surf., B*, 2005, **45**, 167–173.
- 44 S. Doktorovova and E. B. Souto, Nanostructured lipid carrier-based hydrogel formulations for the drug delivery: A comprehensive review, *Expert Opin. Drug Delivery*, 2009, **6**(2), 165–176.
- 45 E. B. Souto and R. H. Muller, The use of SLN and NLC as topical particulate carriers for imidazole antifungal agents, *Pharmazine*, 2006, **61**(5), 431–437.
- 46 S. Shaveta, *et al.*, Development and evaluation of topical gel of curcumin from different combination of polymers formulation and evaluation of herbal gel, *Int. J. Pharm. Pharm. Sci.*, 2012, **4**(4), 452–456.
- 47 S. A. Oluranti, *et al.*, Department of mechanical engineering rheological properties of polymers: Structure and morphology of molten polymer blends, *Mater. Sci. Appli*, 2011, **2**, 30–41.
- 48 Z. Libor, *et al.*, Rheological properties of magnetic and electro-active nanoparticles in non-polar liquids, *J. Mater. Sci.*, 2011, **16**, 5385–5393.
- 49 N. Upendra and G. Neha, Nanostructured lipid carriers (NLC) based controlled release topical gel of clobetasol propionate: design and *in vivo* characterization, *Drug Delivery Transl. Res.*, 2016, **6**(3), 1–10.
- 50 M. Rosanna and O. Thierry, Animal model of atopic dermatitis, *Clin. Dermatol.*, 2003, **21**(2), 122–123.
- 51 H. Jin, *et al.*, Animal models of atopic dermatitis, *J. Invest. Dermatol.*, 2009, **129**, 31–40.
- 52 M. Q. Man, *et al.*, Characterization of a hapten-induced, murine model with multiple features of atopic dermatitis: structural, immunologic, and biochemical changes following single versus multiple oxazolone challenges, *J. Invest. Dermatol.*, 2008, **128**, 79–86.
- 53 H. Kitagaki, *et al.*, Immediate-type hypersensitivity response followed by a late reaction is induced by repeated epicutaneous application of contact sensitizing agents in mice, *J. Invest. Dermatol.*, 1995, **105**, 749–755.
- 54 H. Kitagaki, *et al.*, Repeated elicitation of contact hypersensitivity induces a shift in cutaneous cytokine milieu from a T helper cell type 1 to a T helper cell type 2 profile, *J. Immunol.*, 1997, **159**, 2484–2491.

